

Manuscript Number: ATE-2016-12771R2

Title: Experimental investigations and modelling of a small capacity diffusion-absorption refrigerator in dynamic mode

Article Type: Research Paper

Keywords: Absorption diffusion refrigeration; Dynamic modelling; Matlab Simulink®

Corresponding Author: Professor. Mahmoud Bourouis, Ph.D.

Corresponding Author's Institution: Rovira i Virgili University

First Author: Rami Mansouri, PhD Student

Order of Authors: Rami Mansouri, PhD Student; Mahmoud Bourouis, Ph.D.; Ahmed Bellagi, PhD

Abstract: This paper reports on the experimental investigations in a non-steady state mode of a small capacity commercial diffusion-absorption refrigerator (DAR) and the development of a dynamic black-box model for the machine. For these investigations, the refrigerator was equipped with the appropriate metrology. Temperature time variations of the refrigerated room and of the ambient conditions were measured, monitored, and stored using a data acquisition unit connected to a computer. A standardized experimental procedure was used to determine the overall heat conductance of the refrigerated room: A value of $(UA)_{cab} = 0.554 \text{ WK}^{-1}$ was found. The time evolution of the cooling capacity for different driving heat inputs to the refrigerator was investigated. Based on the experimental data, a dynamic black-box model was developed using the Matlab identification package to correlate the power input to the generator and the cooling capacity of the refrigerator. A first order transfer function with a delay was found to describe quite accurately the time evolution of the cooling capacity for all considered heat rates supplied to the generator. In a further step, regressed analytical expressions of the transfer function parameters, as a function of the generator heat supply, were incorporated into the cooling capacity function. A generalized dynamic black-box model for the DAR system was thus obtained and was then validated using the Matlab Simulink® environment. The predictions made by the model were found to be well in agreement with the experimental data. In particular, the predictions for COP under steady state conditions agreed satisfactorily with the experimental data yielding a maximum relative deviation of about 8%.

Experimental investigations and modelling of a small capacity diffusion-absorption refrigerator in dynamic mode

Rami Mansouri^{a,b}, Mahmoud Bourouis^{b*}, Ahmed Bellagi^a

^a*U. R. Thermique & Thermodynamique des Procédés Industriels
Ecole Nationale d'Ingénieurs de Monastir, ENIM
Avenue Ibn El Jazzar, 5019 Monastir
University of Monastir - Tunisia*

^bDepartment of Mechanical Engineering, Universitat Rovira i Virgili,
Av. Països Catalans No. 26, 43007 Tarragona, Spain

*Corresponding author

Email: mahmoud.bourouis@urv.cat ; Phone: +34 977 55 86 13 ; Fax: +34 977 55 96 91

Abstract

This paper reports on the experimental investigations in a non-steady state mode of a small capacity commercial diffusion-absorption refrigerator (DAR) and the development of a dynamic black-box model for the machine. For these investigations, the refrigerator was equipped with the appropriate metrology. Temperature time variations of the refrigerated room and of the ambient conditions were measured, monitored, and stored using a data acquisition unit connected to a computer. A standardized experimental procedure was used to determine the overall heat conductance of the refrigerated room: A value of $(UA)_{cab} = 0.554 \text{ WK}^{-1}$ was found. The time evolution of the cooling capacity for different driving heat inputs to the refrigerator was investigated. Based on the experimental data, a dynamic black-box model was developed using the Matlab identification package to correlate the power input to the generator and the cooling capacity of the refrigerator. A first order transfer function with a delay was found to describe quite accurately the time evolution of the cooling capacity for all considered heat rates supplied to the generator. In a further step, regressed analytical expressions of the transfer

30 function parameters, as a function of the generator heat supply, were incorporated into the
31 cooling capacity function. A generalized dynamic black-box model for the DAR system
32 was thus obtained and was then validated using the Matlab Simulink® environment. The
33 predictions made by the model were found to be well in agreement with the experimental
34 data. In particular, the predictions for *COP* under steady state conditions agreed
35 satisfactorily with the experimental data yielding a maximum relative deviation of about
36 8%.

37 **Keywords:** Absorption diffusion refrigeration, Dynamic modelling, Matlab Simulink®.

38

39 **Highlights**

40

- 41 ○ Dynamic operation of a small capacity commercial diffusion-absorption refrigerator is
42 experimentally investigated.
- 43 ○ A first order transfer function is used to describe the relationship between the driving
44 power and the cooling capacity.
- 45 ○ A generalized dynamic black-box model for the DAR refrigerator is developed using
46 Matlab Simulink® environment.
- 47 ○ The predictions made by the model for steady-state *COP* are well in agreement with
48 experimental data.

49

50

51 **Nomenclature**

52 COP : Coefficient of performance (-)

53 $F(t)$: Unit step function (-)

54 G_R : Transfer function (-)

55 K_P : Static gain (-)

56 \dot{Q}_{gen} : Generator heating power (W)

57 \dot{Q}_{heat} : Electric cable heating power (W)

58 \dot{Q}_f : Cooling capacity (W)

59 R : Resistance of the electric cable (Ohm)

60 s : Laplace variable (-)

61 T : Temperature ($^{\circ}C$)

62 t : Time (s)

63 U, Y : Laplace transform of input and output (-)

64 (UA) : Overall heat conductance ($W K^{-1}$)

65 τ_d : Time delay (s)

66 θ_p : Time constant (s)

67 φ : Applied voltage (V)

68 **Subscripts**

69 amb : ambient

70 cab : Refrigerated room

71 $elec$: Electric

72 $evap$: Evaporator

73 int : Refrigerator interior

74

75

76

77 1. INTRODUCTION

78 Diffusion absorption refrigeration (DAR) systems are widely used in supermarkets, domestic
79 freezers, and hotel rooms, etc. This technique for producing cold was patented in 1928 by the
80 two Swedish engineers, van Platen and Munters [1]. The unique feature of the DAR cycle,
81 compared to a conventional ammonia/water absorption cycle, is that it operates at a uniform
82 pressure. The working fluid is a mixture of three components: ammonia as a refrigerant, water
83 as an absorbent, and an auxiliary inert gas, frequently hydrogen or helium. The inert gas is
84 necessary to reduce the partial pressure of the refrigerant in the evaporator, and allow for it to
85 evaporate at low temperatures and for the production of useful cold. DAR systems are silent
86 because they have no moving parts.

87 Over the years, investigations have been published on the performance of various
88 configurations of DAR cycles using graphical, numerical and experimental approaches.
89 Kouremenos *et al.* [2] investigated the use of helium as an alternative to hydrogen. The
90 authors observed a similar behaviour of both inert gases. Zohar *et al.* [3] developed a
91 thermodynamic model for an Electrolux DAR system and analysed its performance with both
92 inert gases and found that the *COP* of the system operating with helium was 40% higher than
93 that of the system operating with hydrogen. They further reported that higher *COP* values
94 were obtained by using an ammonia mass fraction of 30% in the rich solution and of 10% in
95 the weak solution. Zohar *et al.* [4] compared the configurations of a DAR cycle both with and
96 without condensate sub-cooling prior to the evaporator entrance. They showed that in the
97 DAR cycle without sub-cooling there was a 14-20% higher *COP* than in the DAR cycle with
98 condensate sub-cooling. Zohar *et al.* [5] examined numerically the performance of a DAR
99 system operating with the organic absorbent DMAC which was associated to five different
100 refrigerants and with helium as an inert gas. They compared the performance of their systems
101 with that of the system operating with ammonia-water and helium and found out that that the

102 latter had the highest *COP* values. Ben Ezzine *et al.* [6] investigated the feasibility of a DAR
103 system operating with the working fluid system DMAC-R124-He and coupled to a solar
104 collector. They reported that both the *COP* and the temperature of the cooling effect depended
105 largely on the effectiveness of the absorber and the generator temperature. For solar cooling
106 applications, this working fluid mixture could be an alternative to the conventional ammonia-
107 water-hydrogen mixture. Starace and De Pascalis [7] developed an enhanced thermodynamic
108 model to consider the more realistic operating conditions of the DAR cycle, such as the
109 presence of some water (absorbent) in the refrigerant stream (ammonia). They used a
110 magnetron activated thermal pump in order to reduce the start-up time of the refrigerator. The
111 model's predictions were validated on a prototype built by coupling a domestic magnetron to
112 a small purposely modified commercial DAR. A maximum deviation was noticed to be
113 roughly 2% in the weak solution mass flow rate and lower than 5% in the *COP* between the
114 predicted and measured data. Sayadi *et al.* [8] presented a HYSYS simulation model for a
115 water-cooled DAR system using different binary mixtures of light hydrocarbons ($C_3/n-C_6$,
116 $C_3/cyclo-C_6$, $C_3/cyclo-C_5$, propylene/cyclo- C_5 , propylene/*i*- C_4 and propylene/*i*- C_5) as working
117 fluids and helium as an inert gas. The driving heat in the generator was supposed to be
118 supplied by evacuated tube solar collectors. The most appropriate binary mixture was found
119 to be $C_3/n-C_6$ with a generation temperature of 126°C. Long *et al.* [9] investigated
120 numerically the possibility of using TFE-TEGDME in the DAR system together with two
121 cooling mediums, namely water at 32 °C and ambient air at 35 °C. The authors performed a
122 parametric analysis on the effects of the cooling medium, the generation and evaporation
123 temperatures and the effectiveness of the absorber on the system performance. They
124 compared the performance of the TFE-TEGDME and NH_3-H_2O DAR systems in terms of
125 *COP* and circulation ratio. They concluded that the TFE-TEGDME mixture is a good
126 working fluid for DAR systems and found that with an absorber effectiveness of 0.8, the

127 optimum generation temperature for the air-cooled TFE–TEGDME DAR system is around
128 170°C. A coefficient of performance (*COP*) up to 0.45 was obtained. However, the
129 performance of the water-cooled system was better with a lower generation temperature of
130 130°C and a higher *COP* of 0.56. Rodriguez-Munoz and Belman-Flores [10] presented a
131 review on diffusion-absorption refrigeration technology in which over 70 publications were
132 analysed. The authors concluded that diffusion-absorption technology represents an
133 interesting and feasible alternative for small capacity refrigeration applications. Rattner and
134 Garimella [11] proposed a fully passive DAR system operating with the working fluid
135 mixture NH₃-NaSCN-He. Detailed design models for the various components of the system
136 were elaborated. They reported *COP*s in the range of 0.11-0.26 at an ambient air temperature
137 of 24°C, low heat source temperatures of 110-130°C and passive air cooling. These authors
138 reported [12] on the development of a prototype of the theoretically investigated machine,
139 activated by low temperature heat sources (110 - 130°C) and passively air-cooled. The
140 cooling temperatures achieved were suitable for refrigeration ($T_{\text{evap}} = 6 \rightarrow 3^{\circ}\text{C}$, *COP* ~ 0.06)
141 and air-conditioning (12 \rightarrow 8°C, *COP* ~ 0.14; 18 \rightarrow 14°C, *COP* ~ 0.17). Chen *et al.* [13]
142 improved the coefficient of performance of the DAR system by 50%. They modified the
143 design and construction of the generator by integrating a tube-in-tube solution heat exchanger
144 into the generator. Vicatos [14] studied experimentally a modified domestic DAR in order to
145 reduce the response time of the system. Koyfman *et al.* [15] presented an experimental
146 investigation on the bubble pump performance in a DAR system. They used a solution of an
147 organic solvent and HCFC as refrigerant. Their results showed that the performance of the
148 bubble pump depends mostly on the motive head and the heat input to the bubble pump. Jacob
149 *et al.* [16] conducted a theoretical and experimental study on a solar driven ammonia-water
150 diffusion absorption cooling machine (DACM). They designed four prototypes for air-
151 conditioning applications: water chillers with an evaporator temperature in the range of 6-

152 12°C and ceiling cooling with an evaporator temperature of 15-18°C. The *COP* values
153 achieved ranged from 0.10 to 0.45. Yıldız and Ersöz [17] designed a DAR system driven by
154 electricity. They investigated numerically and experimentally the energy and exergy losses for
155 each component of the system and compared the theoretical and experimental values. They
156 concluded that the highest exergy losses took place in the solution heat exchanger. The
157 experimental and predicted *COP* was around 0.19 and the exergy efficiency between 0.03 and
158 0.04. Mazouz *et al.* [18] studied experimentally a commercial DAR refrigerator in order to
159 determine its performance under various operating conditions and developed a theoretical
160 simulation model of different DAR configurations.

161 Ben Jemaa *et al.* [19] examined and discussed the relationship between the driving heat and
162 the cooling capacity of a DAR refrigerator in start-up mode. They reported that a transfer
163 function of a first order with a delay is an adequate model to predict the cooling capacity of
164 the refrigerator in steady state mode with a maximum deviation of 8% for different values of
165 the driving heat in the generator.

166 The majority of published works on diffusion absorption refrigeration systems available in the
167 literature deals with steady-state modelling associated or not to experimental tests, but few
168 investigations have been performed on the dynamic behaviour of this kind of refrigeration
169 system. In fact, most of the studies published on the dynamic behaviour of cooling systems
170 [20-28] do not deal with DARs. However, it is of great importance to understand the dynamic
171 operation of these systems. In the present work, a black box dynamic model was developed
172 to predict the refrigerator performance in terms of cooling capacity and *COP*. The model
173 was based on experimental measurements taken from a small capacity commercial
174 diffusion-absorption refrigerator. The specific objectives are as follows:

- 175 i. Experimental characterization of a small capacity commercial diffusion-absorption
176 refrigerator in dynamic mode.

177 ii. Development and validation of a detailed black-box model for this refrigerator, based on
178 the experimental data and using Matlab Simulink® environment.

179

180 **2. Working principle**

181 A 3-D scheme of the investigated refrigerator is presented in Fig. 1. It is a small capacity
182 refrigerator of 44 litres and internal dimensions of 490 mm x 360 mm x 250 mm (height x
183 width x depth), designed for hotel rooms, activated by an electric heater, and operating with
184 the ternary fluid mixture ammonia-water-hydrogen. The machine has of a generator which
185 consists of a combined bubble pump and a boiler, a rectifier, a condenser, an evaporator, a gas
186 heat exchanger (GHX), an absorber, a solution heat exchanger (SHX) and a solution tank.

187 The generator contains initially a rich ammonia-water solution. When sufficient heat is
188 supplied, ammonia vapour is generated and moves up through the vertical bubble pump tube
189 carrying the liquid solution with it. At the top of the bubble pump the ammonia solution and
190 ammonia vapour are separated. The liquid solution falls in the boiler and continues further on to
191 the absorber by force of gravity. The vapour flows to the condenser, where it condenses. The
192 ammonia liquid flows further to the evaporator where it meets hydrogen coming from the
193 absorber. Its partial pressure is so decreased that the liquid begins to evaporate by taking heat
194 from the refrigerated space. After leaving the evaporator, the gaseous mixture is conducted
195 through the annulus of the tube-in-tube gas heat exchanger (GHX) to ensure that it pre-cools
196 the liquid refrigerant and the hydrogen-rich gas flowing counter-currently on their way up to
197 the evaporator. The mixture of refrigerant and hydrogen flows further down to the absorber
198 inlet. In the absorber, the ammonia vapour is absorbed by the ammonia-weak solution returning
199 from the generator, transforming it to an ammonia-rich solution, which is collected in the
200 solution tank. From there it starts its way to the bubble pump via the solution heat exchanger
201 (SHX) and then back to the generator.

202 3. Experimental characterization of the dynamic operation of the refrigerator

203 To experimentally investigate the functioning of the DAR system in dynamic mode, the
204 refrigerator was equipped with 11 K-thermocouples placed at the entrance and exit of each of
205 its components and connected via a data acquisition unit (34970A AGILENT) to a computer
206 (Fig. 2) where the experimental data were collected and saved. The thermocouples were
207 calibrated beforehand using an ice-water bath. A fluctuation in the temperature of $\pm 0.5^\circ\text{C}$ was
208 noticed. The electric heating system was connected to a power controller (Fig. 2). The
209 experimental tests were carried out by first adjusting the heating power to the generator, \dot{Q}_{gen} ,
210 then measuring the temperatures and storing the data all the time, from the start-up until the
211 steady-state regime was reached. The thermostat was disconnected so that the refrigerator was
212 operated in a continuous mode and an air-conditioned environment at a set point temperature
213 of 24°C . It is worthy of note that the experimental procedure employed in the present work
214 doesn't follow any protocol of the standards developed for laboratory testing of household
215 refrigerators [29-34]. The experiments were performed with different heat supplies \dot{Q}_{gen} to
216 the generator, namely 35, 39, 44, 46, 48, 51, 53, 56, 58, 61 and 67 W. Fig. 3 shows the time
217 evolution of the liquid stream temperature at the generator exit for the two lowest values of
218 the energy supply to the machine. For $\dot{Q}_{gen} = 35\text{W}$, the temperature exhibits an oscillatory
219 behaviour: it fluctuates between 205°C and 155°C with a time period of 100 minutes. This
220 heat supply ensures the functioning of the refrigerator, but not its stability. With a little
221 increase in the heat supply, $\dot{Q}_{gen} = 39\text{W}$, some fluctuations are initially observed. They then
222 cease after 150 minutes, leading to a steady-state operation with the temperature of the
223 solution leaving the generator stabilizing at 158°C . In fact, when the heating power supplied
224 to the generator was not sufficient, the bubble pump did not reach steady operation point. The
225 large vapour bubbles responsible for the pumping of the liquid were not continuously formed.
226 Although ammonia vapour was generated, the flow regime was almost bubbly and the liquid

227 was only occasionally conveyed upwards. With increasing heat supply, a stable plug flow
 228 regime was reached and the steady pumping of the liquid was ensured. Moreover, increasing
 229 the heat power supply to the generator \dot{Q}_{gen} from 44W to 67W the initial fluctuations of the
 230 solution temperature at the generator exit were attenuated (Fig. 4(a)) and the time required by
 231 the refrigerator to reach a steady-state regime reduced (Fig. 4(b)) at a given temperature of the
 232 refrigerated room. Fig. 5 shows how the temperatures at the evaporator inlet and outlet and in
 233 the refrigerated room respond to four different values of the energy supply \dot{Q}_{gen} in the range
 234 of 39-67W. It is worthy of note that in the case of $\dot{Q}_{gen} = 39\text{W}$, the temperatures at the inlet
 235 and outlet of the evaporator are very far apart (-22°C vs. -5°C) and that the temperature at the
 236 inlet fluctuates largely between $+10$ and -22°C .

237 To evaluate the cooling capacity of the refrigerator, $\dot{Q}_f(t)$, the overall heat conductance
 238 $(UA)_{cab}$ of the refrigerated room is needed. For the present study, it was determined by
 239 applying a standardized procedure in a separate test set. To this purpose, the refrigerated room
 240 of the refrigerator was heated by an electric resistance cable ($R = 135\Omega$) placed inside. This
 241 heater was connected to a power controller in order to vary the electric power supplied. Seven
 242 tests were performed by varying the voltage φ applied to the resistor, namely φ : 17, 20, 22,
 243 26, 28, 30 and 32 V. For each test, the indoor and outdoor temperatures were measured. When
 244 steady-state regime is reached, the indoor temperature becomes constant, i.e. the heat

245 generated in the electric resistance cable $\dot{Q}_{heat} = \left[\varphi^2 / R \right]$ is equal to the total heat losses \dot{Q}_{loss}

246 from the refrigerated room (Eq. 1):

$$247 \quad \dot{Q}_{loss} = (UA)_{cab}(T_{int} - T_{amb}) \quad (1)$$

248 It follows then:

$$249 \quad (UA)_{cab} = \frac{\dot{Q}_{heat}}{(T_{int} - T_{amb})} = \frac{\left[\varphi^2 / R \right]}{(T_{int} - T_{amb})} \quad (2)$$

250 The experiment was repeated for seven different values of \dot{Q}_{heat} . The slope of the regression
251 line representing $\left[\frac{\varphi^2}{R}\right]$ vs. $(T_{int} - T_{amb})$, shown in Fig. 6, leads to an average value of
252 $(UA)_{cab} = 0.55 \text{ WK}^{-1}$, with an absolute uncertainty of $\pm 0.01 \text{ WK}^{-1}$.

253 The material properties of the refrigerated room walls and the thermo-physical properties of
254 ambient air outside the refrigerator were constant during the tests and the mean properties of
255 air inside the refrigerator can be assumed roughly unchanged, so the obtained value of
256 $(UA)_{cab}$ was used to determine the instantaneous cooling capacity $\dot{Q}_f(t)$ from the start-up of
257 the refrigerator till it reaches a steady-state regime (Eq. 3), the relative uncertainty being
258 around 4%.

$$259 \quad \dot{Q}_f(t) = (UA)_{cab}(T_{int}(t) - T_{amb}) \quad (3)$$

260

261 **4. Dynamic black-box modelling of the refrigerator**

262 Very often process models are developed from knowledge gained of the underlying process
263 mechanisms and they describe the physicochemical processes taking place in the system.
264 These mechanistic models known as "white boxes" are developed for design and optimization
265 applications.

266 Contrarily, empirical models are solely the result of experiments and observation and do
267 usually not rely on the knowledge of basic principles and mechanisms. Equation fitting is then
268 employed to determine the model parameters, which have little or no physical meaning. These
269 so-called "black box" models are of purely descriptive nature and with limited ranges of
270 application however, they do constitute helpful tools for process control and automation
271 purposes.

272 In this kind of modelling, the pertinent information for model identification is obtained
273 through exciting or stimulating the system. Structure and parameter estimation methods

274 developed in the field of process identification are then used to establish the model. These two
275 steps are however, not really independent, as the criterion of the choice of a model from a set
276 of candidates with unknown parameters is the best fit for the measured data.

277 In the choice of a black-box model for a DAR system, one should keep in mind requirements
278 for good model structure, namely:

- 279 • Simplicity—in its mathematical form,
- 280 • Generality—in its ability to describe the refrigerator behaviour for all power inputs.

281 282 **4.1 Mathematical model**

283 The model developed is based on some simplifying assumptions.

- 284 • First, the ambient temperature is supposed constant. This takes in account the fact that the
285 tests are performed in a temperature-controlled room, with a temperature varying between
286 24 and 26°C.
- 287 • Second, the steady-state values of the overall heat conductance $(UA)_{cab}$ are supposed to
288 be the same in transient mode. This means that the latent heat contribution during the
289 start-up is neglected, as the steady state $(UA)_{cab}$ -value accounts only for sensible load.
- 290 • Further, at constant ambient temperature, the heating power supplied to the generator is
291 the only input that affects the operation of the refrigeration unit. Hence, the input signal to
292 the system is $\dot{Q}_{gen}(t)$:

$$293 \quad \dot{Q}_{gen}(t) = \dot{Q}_{gen} F(t) \quad (4)$$

294 where $F(t)$ is the unit step function.

295 The system response to this input is the cooling effect $\dot{Q}_f(t)$ achieved in the refrigerated
296 room. In terms of system theory, the used DAR unit is then a single-input, single-output
297 (SISO) system. To establish a dynamic black-box model of the refrigerator, nine (repeated)
298 tests were carried out using different inputs, i.e. the heat supply to the generator of the

299 refrigerator $\dot{Q}_{gen}(t)$, and the response of the system, i.e. the time evolution of the cooling
 300 effect $\dot{Q}_f(t)$, noticed. As mentioned before, the next two steps in the elaboration of a model
 301 are the model structure and the estimation of model parameters. In the present work, these
 302 steps were performed by analysing the experimental input and output data using the software
 303 MATLAB and its system identification package. It was found that the most adequate dynamic
 304 model for the description of the time evolution of $\dot{Q}_f(t)$ for every chosen energy supply \dot{Q}_{gen}
 305 corresponds to the response of a first order system with a delay. Fig. 7 illustrates this finding
 306 in the case of the four values of $\dot{Q}_{gen}=44\text{W}$, $\dot{Q}_{gen}=48\text{W}$, $\dot{Q}_{gen}=51\text{W}$ and $\dot{Q}_{gen}=53\text{W}$. This
 307 means that the transfer function $G_R(s)$ of the DAR refrigerator is in the form:

$$308 \quad G_R(s) = \frac{K_P}{1+\theta_p s} e^{-\tau_d s} \quad (5)$$

309 where K_P is the static gain, θ_p the time constant and τ_d the time delay. When applied to our
 310 machine data this simple three-parameter model describes quite accurately the time evolution
 311 of the cooling capacity for all values of the heat power supply to the generator as shown in
 312 Fig. 7. The fitting quality, an indicator of the quality of the regression results, ranges from
 313 90% to 98%.

314 The transfer function that relates the rate of heat supply \dot{Q}_{gen} as an input signal and the
 315 cooling capacity $\dot{Q}_f(t)$ as an output signal is:

$$316 \quad G_R(s) = \frac{Y(s)}{U(s)} = \frac{K_P}{1+\theta_p s} e^{-\tau_d s} \quad (6)$$

317 with $U(s)$ is the Laplace transform of $\dot{Q}_{gen}(t)$,

$$318 \quad U(s) = \mathcal{L}[\dot{Q}_{gen}F(t)] \quad (7)$$

319 and $Y(s)$ the Laplace transform of the cooling capacity $\dot{Q}_f(t)$,

$$320 \quad Y(s) = \mathcal{L}[\dot{Q}_f(t)] \quad (8)$$

321 The time domain of the cooling capacity $\dot{Q}_f(t)$ can be deduced from equation (6),

$$322 \quad \dot{Q}_f(t) = \dot{Q}_{gen} K_P (1 - e^{\frac{-t-\tau_d}{\theta_p}}) F(t - \tau_d) \quad (9)$$

323 Fig. 7 shows the calculated time evolution of $\dot{Q}_f(t)$ in comparison with the experimental
324 curves for the indicated values of the heating power supply to the generator. It can be
325 appreciated that the black-box model reproduces quite accurately the unsteady-state
326 performance of the DAR refrigerator.

327 Table 1 summarizes the model parameters and the fitting quality indicator for all investigated
328 values of \dot{Q}_{gen} .

329 **4.2 Generalized black-box dynamic model & validation**

330 The analysis of the results in Table 1 reveals that the three model parameters K_P , θ_p and τ_d
331 depend on the heat input \dot{Q}_{gen} . This dependency is graphically depicted in Figs. 8, 9 and 10
332 with dots representing the values of the parameters and continuous lines their least-square
333 fitted curves. If the corresponding regression relations $K_P(\dot{Q}_{gen})$, $\theta_p(\dot{Q}_{gen})$ and $\tau_d(\dot{Q}_{gen})$
334 are incorporated into the expression of $\dot{Q}_f(t)$ (Eq. 9), one obtains a generalized model of the
335 DAR refrigerator, i.e. a function $\dot{Q}_f(t, \dot{Q}_{gen})$ which predicts the instantaneous evolution of
336 the cooling capacity for every heating power supply to the generator within the range
337 investigated.

338 The test for this generalized black-box dynamic model of the DAR refrigerator was run using
339 the software package MATLAB SIMULINK® (Fig. 11). The time evolution of the cooling
340 capacity calculated by both the specific and generalized models in comparison with
341 experimental data describes reasonably well the dynamic behaviour of the DAR refrigerator
342 and predicts fairly well the unsteady-state performance of the refrigerator. The fitting quality
343 of the generalized model for the different inputs \dot{Q}_{gen} ranges between 84% and 94%.

344 Fig. 12 shows a further test on the black-box models. It represents a comparison between the
345 experimental cooling capacity and its calculated values for different values of \dot{Q}_{gen} and for
346 both the heat-rate-specific and generalized dynamic models. As can be seen, both models
347 satisfactorily predict the cooling capacity of the used DAR refrigerator when steady-state
348 regime is reached. Table 2 summarizes the relative deviations in predicting the cooling
349 capacity at the different heat rates supplied to the generator. The maximum relative error is
350 8.2% and 7.5% for the specific and generalized models, respectively.

351 The experimental steady-state coefficient of performance (COP) values of the DAR (Eq. 9),
352 predicted for different heat supplies to the generator by both models are well in agreement
353 with the experimental data. The maximum relative deviation in COP prediction is about 8%.

$$354 \quad COP = \frac{\dot{Q}_{evap}}{\dot{Q}_{gen}} \quad (9)$$

355 Therefore, it can be concluded that both specific and generalized black-box models predict the
356 cooling capacity and the coefficient of performance of the DAR refrigerator well when a
357 steady-state regime is reached.

358 5. Conclusion

359 In the present work, experimental investigations were carried out on the operation of a small
360 capacity commercial diffusion-absorption refrigerator (DAR) at an unsteady-state regime and
361 a dynamic black-box model was developed for the refrigerator. The results of these
362 investigations can be summarized as follows:

- 363 • A heat supply to the generator of over 35 W is required to ensure the functioning of the
364 commercial DAR refrigerator and its stability.

- 365 • The standardized experimental procedure used to determine the overall heat conductance
366 of the refrigerated room leads to an average value of $(UA)_{cab} = 0.554 \text{ WK}^{-1}$.
- 367 • A first order transfer function with a delay correctly describes the relationship between the
368 power input to the generator and the cooling capacity as a response of the machine. A
369 maximum relative deviation of about 8.2% between the predicted values by the model and
370 the experimental data was noted.
- 371 • A generalized black-box model was then built by integrating analytical expressions of the
372 three parameters of the model as function of the heat power supplied to the generator in
373 the original specific model.
- 374 • Simulations with the obtained generalized model using Matlab Simulink® environment
375 show that the predictions made by the model deviate by a maximum of 8% from the
376 experimental data.
- 377 • The steady-state *COP* is also well predicted by the generalized black-box model.

378

379

380

381

382

383

384

385

386

387

388

389 **References**

- 390 [1] B.C. Von Platen, C.G. Munters. US Patent 1, 685,764, 1928.
- 391 [2] D.A. Kouremenos, A. Stegou-Sagia. Use of helium instead of hydrogen in inert gas
392 absorption refrigeration. *International Journal of Refrigeration*, 1988, 11, 6-341.
- 393 [3] A. Zohar, M. Jelinek, A. Levy, I. Borde. Numerical investigation of a diffusion
394 absorption refrigeration cycle. *International Journal of Refrigeration*, 2005, 28 (4), 515-
395 525.
- 396 [4] A. Zohar, M. Jelinek, A. Levy, I. Borde. The influence of diffusion absorption refrigeration
397 cycle configuration on the performance. *Applied Thermal Engineering*, 2007, 27 (13),
398 2213-2219.
- 399 [5] A. Zohar, M. Jelinek, A. Levy, I. Borde. Performance of diffusion absorption
400 refrigeration cycle with organic working fluids. *International Journal of Refrigeration*,
401 2009, 32 (6), 1241-1246.
- 402 [6] N. Ben Ezzine, R. Garma, A. Bellagi. A numerical investigation of a diffusion-
403 absorption refrigeration cycle based on R124-DMAC mixture for solar cooling. *Energy*,
404 2010,35 (5), 1874-1883.
- 405 [7] G. Starace, L. De Pascalis. An advanced analytical model of the Diffusion Absorption
406 Refrigerator cycle. *International Journal of Refrigeration*, 2012, 35 (7), 605-612.
- 407 [8] Z. Sayadi, N. Ben Thameur, M. Bourouis, A. Bellagi. Performance optimization of solar
408 driven small air-cooled absorption–diffusion chiller working with light hydrocarbons.
409 *Energy Conversion and Management*, 2013,74, 299-307.
- 410 [9] Z. Long, Y. Luo, H. Li, X. Bu, W. Ma. Performance analysis of a diffusion absorption
411 refrigeration cycle working with TFE–TEGDME mixture. *Energy Building*, 2013,58,
412 86-92.

- 413 [10] J.L. Rodríguez-Muñoz, J.M. Belman-Flores. Review of diffusion-absorption
414 refrigeration technologies. *Renewable and Sustainable Energy Reviews*, 2014, 30, 145-
415 153.
- 416 [11] A.S. Rattner, S. Garimella. Low-source-temperature diffusion absorption refrigeration.
417 Part I: Modeling and cycle analysis. *International Journal of Refrigeration*, 2016, 65,
418 287-311.
- 419 [12] A.S. Rattner, S. Garimella. Low-source-temperature diffusion absorption refrigeration.
420 Part II: Experiments and model assessment. *International Journal of Refrigeration*,
421 2016, 65, 312-329.
- 422 [13] J. Chen, K.J. Kim, K.E. Herold. Performance enhancement of a diffusion absorption
423 refrigerator. *International Journal of Refrigeration*, 1996, 19 (3), 208-218.
- 424 [14] G. Vicatos. Experimental investigation on a three-fluid absorption refrigeration machine.
425 *Journal of Process Mechanical Engineering*, 2000, 214, 157-172.
- 426 [15] A. Koyfman, M. Jelinek, A. Levy, I. Borde. An experimental investigation of bubble
427 pump performance for diffusion absorption refrigeration system with organic working
428 fluids. *Applied Thermal Engineering*, 2003, 23 (15), 1881-1894.
- 429 [16] U. Jakob, U. Eicker, D. Schneider, A.H. Taki, M.J. Cook. Simulation and experimental
430 investigation into diffusion absorption cooling machines for air-conditioning
431 applications. *Applied Thermal Engineering*, 2008, 28 (10), 1138-1150.
- 432 [17] A. Yıldız, M.A. Ersöz. Energy and exergy analyses of the diffusion absorption refrigeration
433 system. *Energy*, 2013, 60, 407-415.
- 434 [18] S. Mazouz, R. Mansouri, A. Bellagi. Experimental and thermodynamic investigation of
435 an ammonia/water diffusion absorption machine. *International Journal of Refrigeration*,
436 2014, 45, 83-91.

- 437 [19] R. Ben Jemaa, R. Mansouri, A. Bellagi. Dynamic testing and modeling of a diffusion
438 absorption refrigeration system. *International Journal of Refrigeration*, 2016, 67, 249-
439 258.
- 440 [20] D. Butz, K. Stephan. Dynamic Behavior of an Absorption Heat Pump. *International*
441 *Journal of Refrigeration*, 1989, 12 (4), 204- 212.
- 442 [21] S. Jeong, B. H. Kang, S. W. Karng. Dynamic Simulation of an Absorption Heat Pump
443 for Recovering Low Grade Waste Heat. *Applied Thermal Engineering*, 1998, 18 (1-2),
444 1-12.
- 445 [22] D. G. Fu, G. Poncia, Z. Lu. Implementation of an Object-Oriented Dynamic Modeling
446 Library for Absorption Refrigeration Systems. *Applied Thermal Engineering*, 2006, 26
447 (2-3), 217-225.
- 448 [23] B. Kim, J. Park. Dynamic Simulation of a Single-Effect Ammonia–Water Absorption
449 Chiller. *International Journal of Refrigeration*. 2007, 30 (3), 535-545.
- 450 [24] P. Kohlenbach, F. Ziegler. A Dynamic Simulation Model for Transient Absorption
451 Chiller Performance. Part I: The Model. *International Journal of Refrigeration*, 2008a,
452 31 (2), 217-225.
- 453 [25] P. Kohlenbach, F. Ziegler. A Dynamic Simulation Model for Transient Absorption
454 Chiller Performance. Part II: Numerical Results and Experimental Verification.
455 *International Journal of Refrigeration*, 2008b, 31 (2), 226-233.
- 456 [26] H. Matsushima, T. Fujii, T. Komatsu, A. Nishiguchi. Dynamic Simulation Program
457 with Object-Oriented Formulation for Absorption Chillers (Modelling, Verification, and
458 Application to Triple-Effect Absorption Chiller). *International Journal of Refrigeration*,
459 2010, 33 (2), 259-268.

- 460 [27] W. Cai, M. Sen, S. Paolucci. Dynamic Simulation of an Ammonia-Water Absorption
461 Refrigeration System. *Industrial & Engineering Chemistry Research*, 2011, 51, 2070-
462 2076.
- 463 [28] M. Zinet, R. Rulliere, P. Haberschill. A Numerical Model for the Dynamic Simulation
464 of a Recirculation Single-Effect Absorption Chiller. *Energy Conversion and*
465 *Management*, 2012, 62, 51-63.
- 466 [29] Indian Standard ICS 97.040.30. Household frost-free refrigerating appliances -
467 Refrigerators cooled by internal forced air circulation - Characteristics and test methods
468 - Specification. Bureau of Indian Standards, New Delhi, December 2006.
- 469 [30] APEC 1999. Review of energy efficiency test standards and regulations in APEC
470 member economies. Published for APEC Secretariat, Singapore, APEC report 99-RE-
471 01.5, ISBN 0-646-38672-7, November 1999, Available electronically from
472 www.energyefficient.com.au.
- 473 [31] AS/NZS 4474.1. Performance of household electrical appliances - Refrigerating
474 appliances - Energy consumption and performance. 1997, Available for purchase from
475 www.standards.com.au.
- 476 [32] AS/NZS 4474.2. Performance of household electrical appliances - Refrigerating
477 appliances - Energy labelling and minimum energy standard requirements. 2000,
478 Available from www.standards.com.au.
- 479 [33] A report on independent laboratory testing of household refrigerator and freezers in
480 Australia. The National Appliance and Equipment Energy Efficiency Committee,
481 March 2001.
- 482 [34] C. Barthel, T. Götz. Test procedures, measurements and standards for refrigerators and
483 freezers. Wuppertal Institute for Climate, Environment and Energy, Germany,
484 December 2012.

485 **Table captions**

486 Table 1. Model parameters and fitting quality for all investigated values of \dot{Q}_{gen} .

487 Table 2. Relative deviation in predicting the cooling capacity for both heat-rate-specific and
488 generalized models.

489

490

491

492

493

494

495

496

497

498

499

500

501

502

503

504

505 Table 1. Model parameters and fitting quality for all investigated values of \dot{Q}_{gen} .

506

\dot{Q}_{gen} (W)	K_p	τ_d	θ_p	Fit (%)
44	0.1395	78.927	66.829	93.91
46	0.1450	71.546	66.618	91.27
48	0.1354	72.092	57.055	94.16
51	0.1253	63.109	57.24	93.08
53	0.1120	60.232	52.523	98.36
56	0.1156	69.676	55.609	93.44
58	0.1096	67.327	54.474	96.90
61	0.0965	56.378	41.623	89.86
67	0.0947	71.510	45.930	95.41

513

514 Table 2. Relative deviation in predicting the cooling capacity for both heat-rate-specific and
515 generalized models.

516

\dot{Q}_{gen} (W)	Cooling capacity (W) <i>Experimental</i>	Cooling capacity (W) <i>Specific model</i>	Relative deviation (%)	Cooling capacity (W) <i>Generalized model</i>	Relative deviation (%)
44	6.43	6.09	5.4	6.10	5.4
46	6.06	6.56	8.2	6.45	6.3
48	6.14	6.24	1.5	6.25	1.8
51	6.64	6.32	5.0	6.32	5.0
53	5.56	5.47	1.8	5.82	4.7
56	6.44	6.43	0.2	6.21	3.7
58	6.10	6.10	0.1	5.97	2.1
61	6.15	5.82	5.8	6.11	0.7
67	6.44	6.16	4.4	5.98	7.5

517

518

519

520

521

522

523

524

525

526 **Figure captions**

527 Fig. 1. Schematic view of the diffusion-absorption refrigerator.

528 Fig. 2. Picture of the refrigerator investigated together with the auxiliary experimental
529 equipment.

530 Fig. 3. Time evolution of the temperature of the weak solution leaving the generator for
531 $\dot{Q}_{gen} = 35\text{W}$ and 39W .

532 Fig. 4. (a) Time evolution of the temperature of the weak solution leaving the generator
533 for $\dot{Q}_{gen} = 44 - 67\text{ W}$; (b) Time required by the refrigerator to reach a steady-state regime
534 vs. heat supply to the generator at a given temperature of the refrigerated room.

535 Fig. 5. Time evolution of the ambient air, refrigerated room and evaporator temperatures at
536 different heat supplies to the generator.

537 Fig. 6. $\left[\frac{\varphi^2}{R} \right]$ vs. $(T_{int} - T_{amb})$.

538 Fig. 7. Time evolution of the cooling capacity determined from experimental measurements
539 and of the heat-rate-specific black box model at different heat supplies to the generator.

540 Fig. 8. K_P vs. \dot{Q}_{gen} .

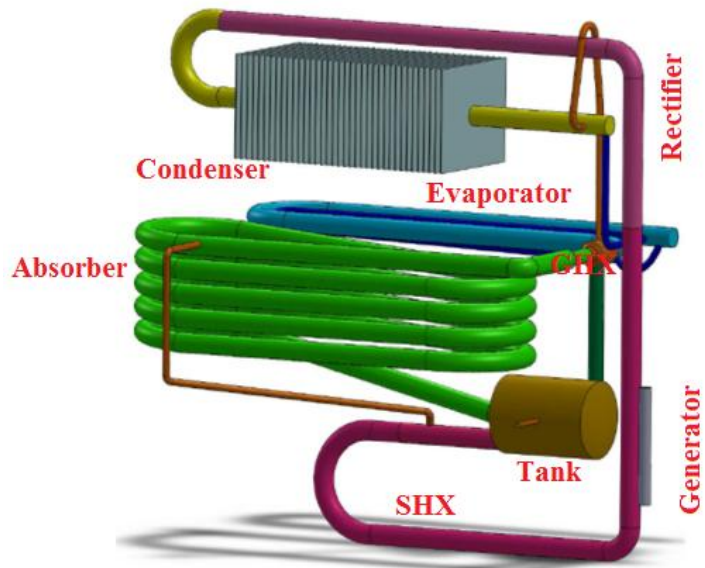
541 Fig. 9. τ_d vs. \dot{Q}_{gen} .

542 Fig. 10. θ_P vs. \dot{Q}_{gen} .

543 Fig. 11. Schematic diagram of the black-box dynamic model in the Matlab Simulink®
544 environment.

545 Fig. 12. Comparison of the experimental steady-state cooling capacity and that predicted by
546 both the heat-rate-specific and generalized models as a function of the heat supply to the
547 generator.

548



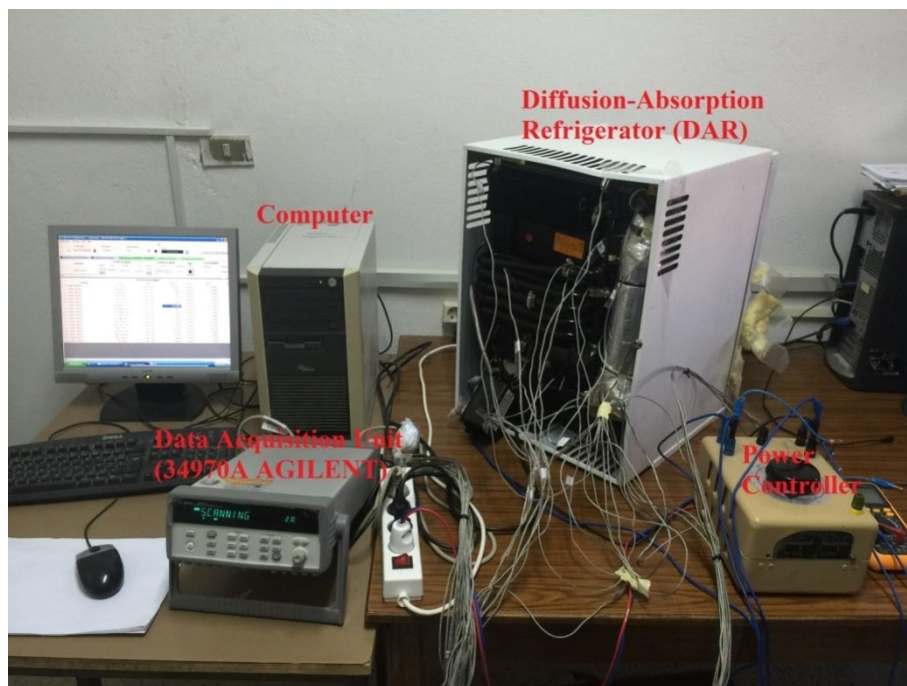
549

550

551

Fig. 1. Schematic view of the diffusion-absorption refrigerator.

552



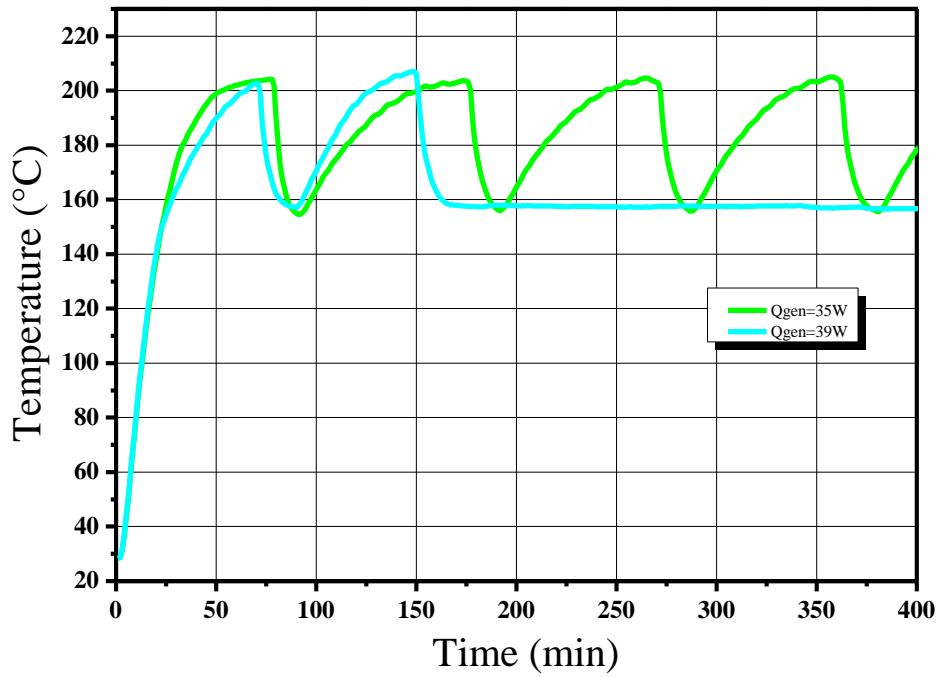
553

554

555

Fig. 2. Picture of the refrigerator investigated together with the auxiliary experimental equipment.

556



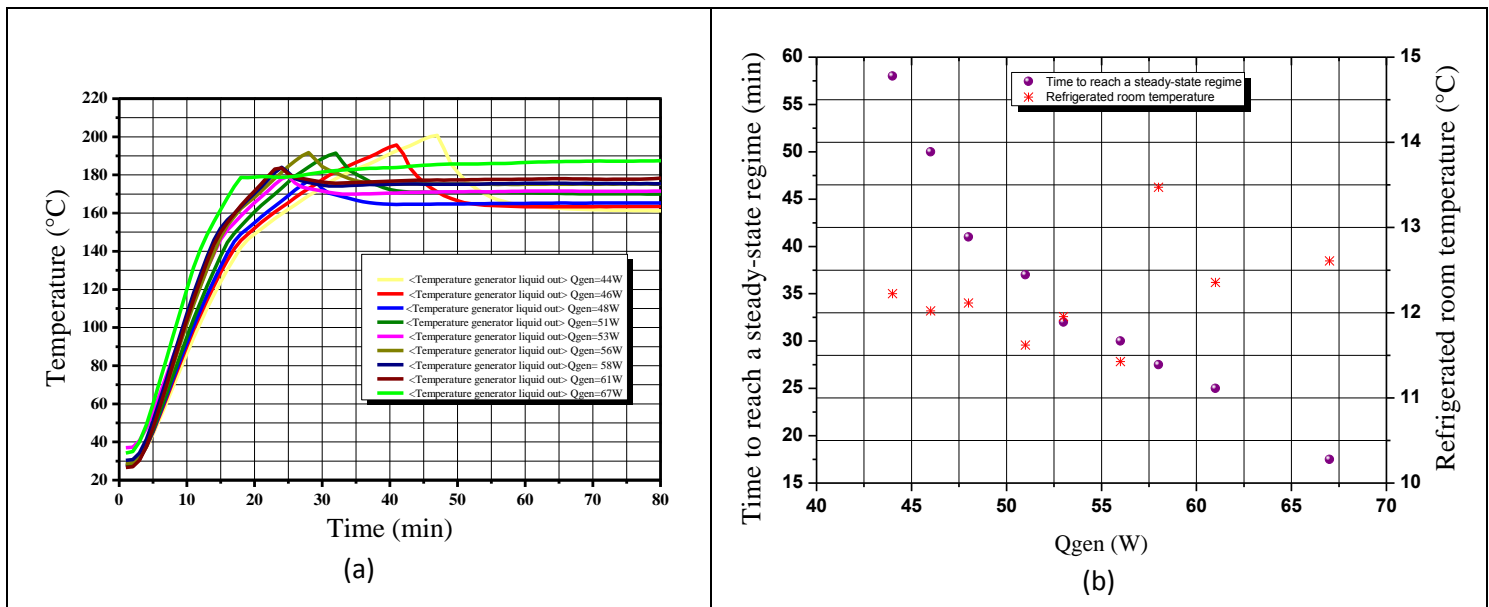
557

558

559 Fig. 3. Time evolution of the temperature of the weak solution leaving the generator for

560

$$\dot{Q}_{gen} = 35W \text{ and } 39W.$$

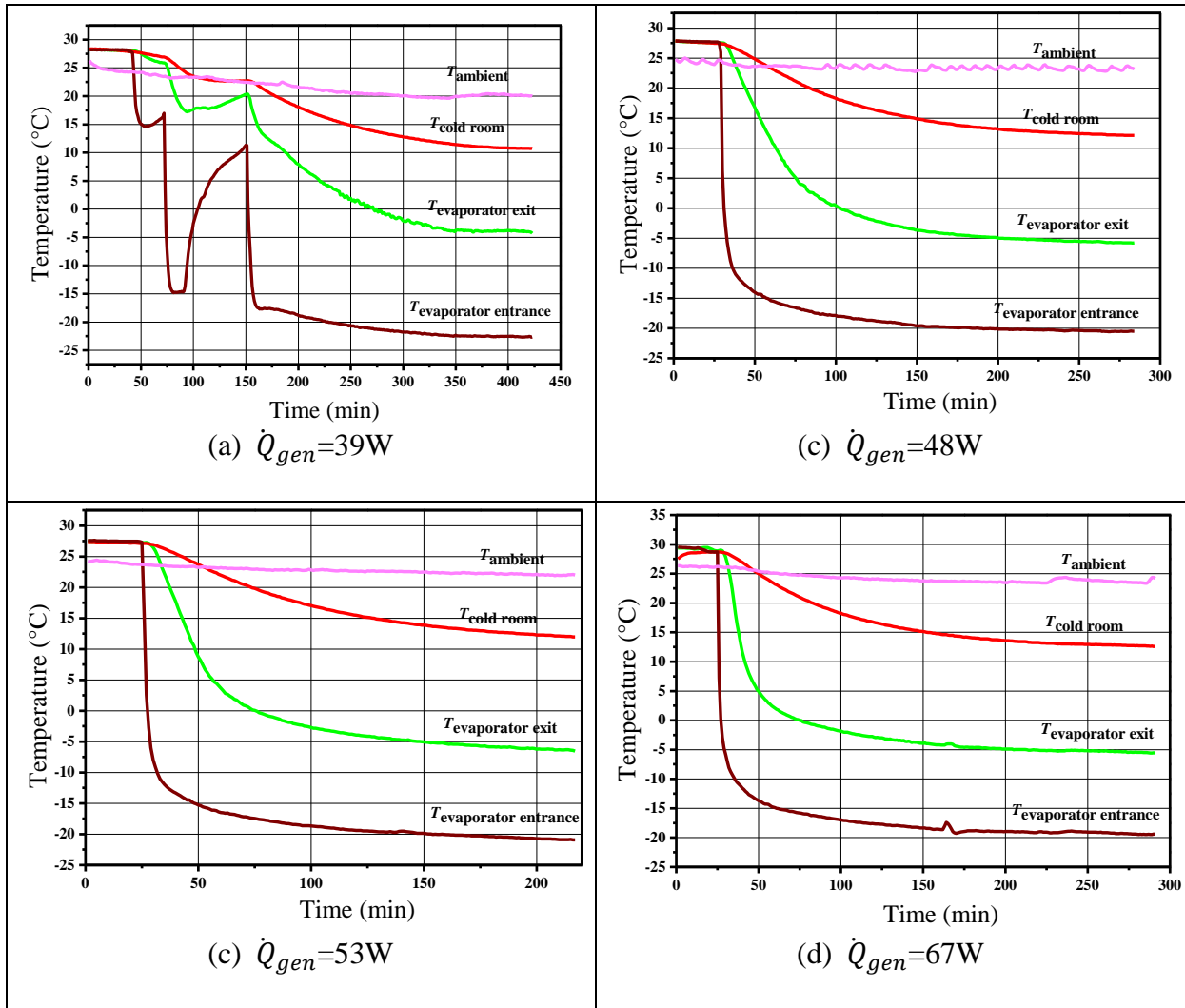


561

562 Fig. 4. (a) Time evolution of the temperature of the weak solution leaving the generator

563 for $\dot{Q}_{gen} = 44 - 67 W$; (b) Time required by the refrigerator to reach a steady-state regime

564 vs. heat supply to the generator at a given temperature of the refrigerated room.



565

566 Fig. 5. Time evolution of the ambient air, refrigerated room and evaporator temperatures at
 567 different heat supplies to the generator.

568

569

570

571

572

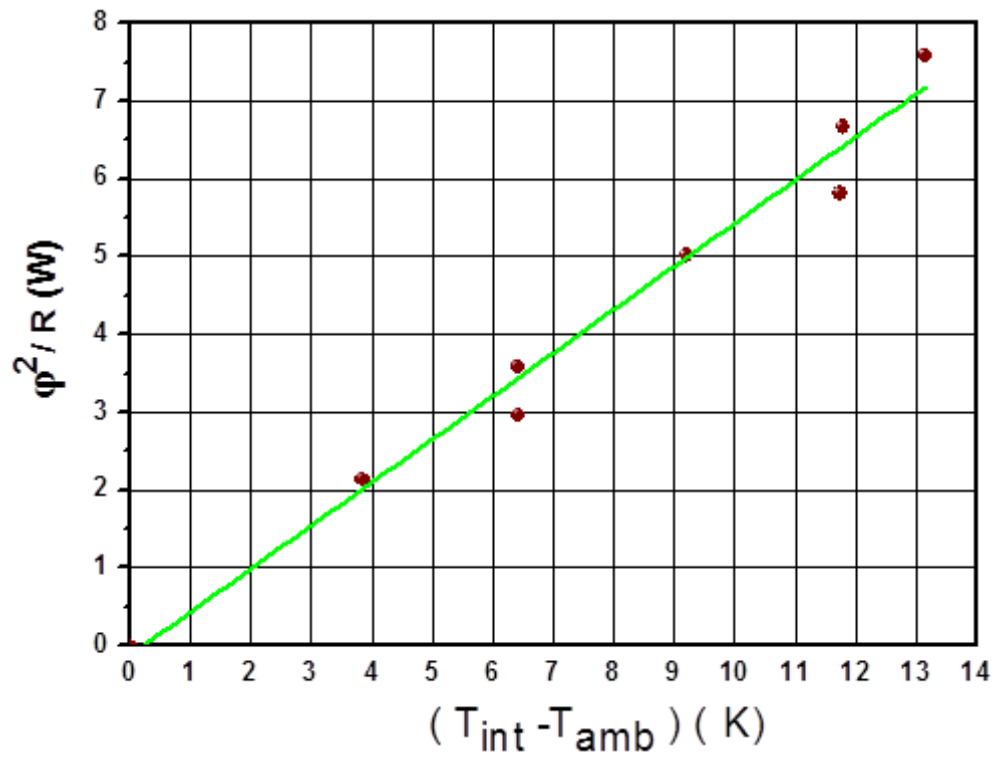
573

574

575

576

577



578

579

Fig. 6. $\left[\phi^2 / R \right]$ vs. $(T_{int} - T_{amb})$.

580

581

582

583

584

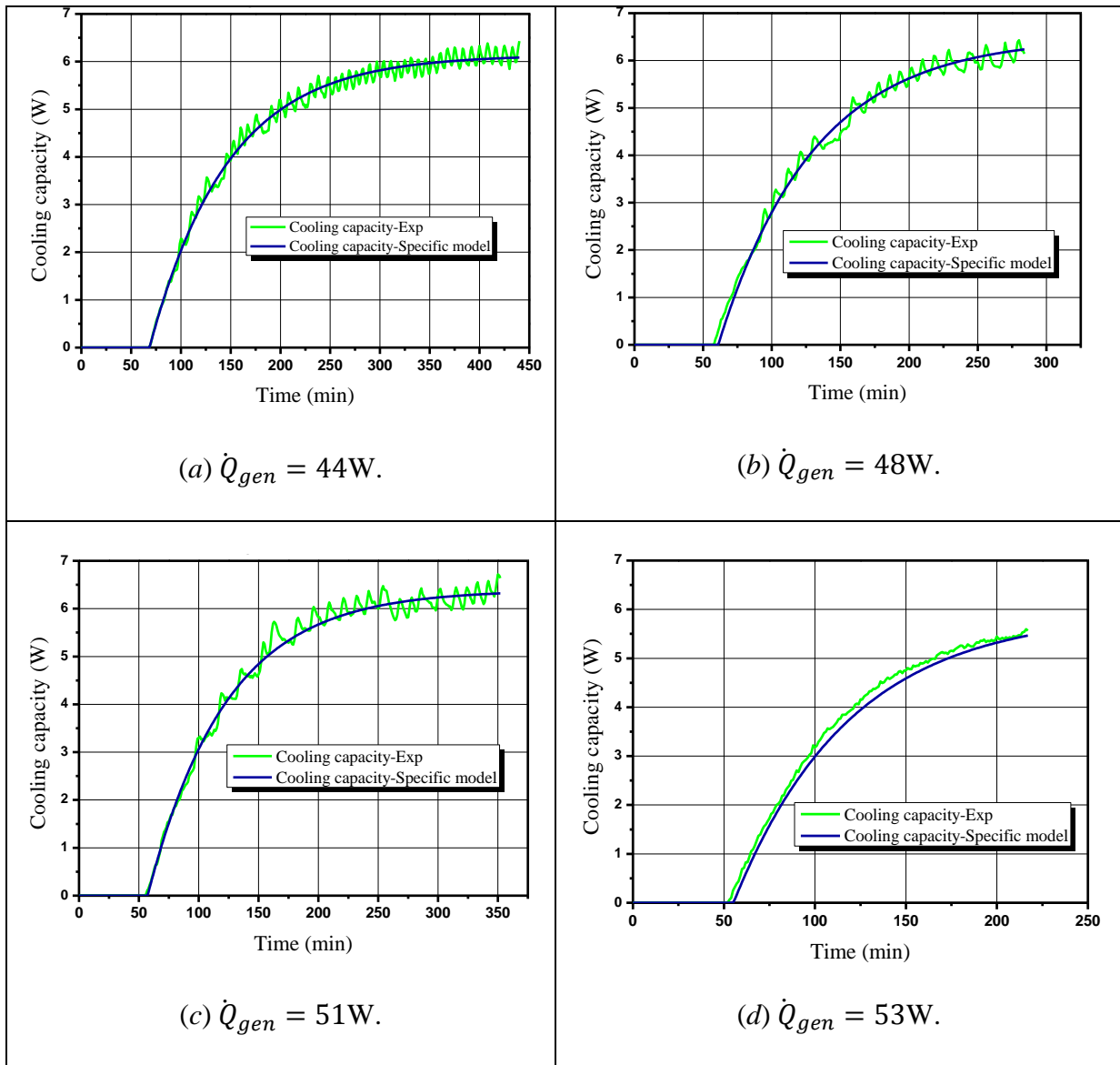
585

586

587

588

589



590

591 Fig. 7. Time evolution of the cooling capacity determined from experimental measurements
 592 and the heat-rate-specific black box model at different heat supplies to the generator.

593

594

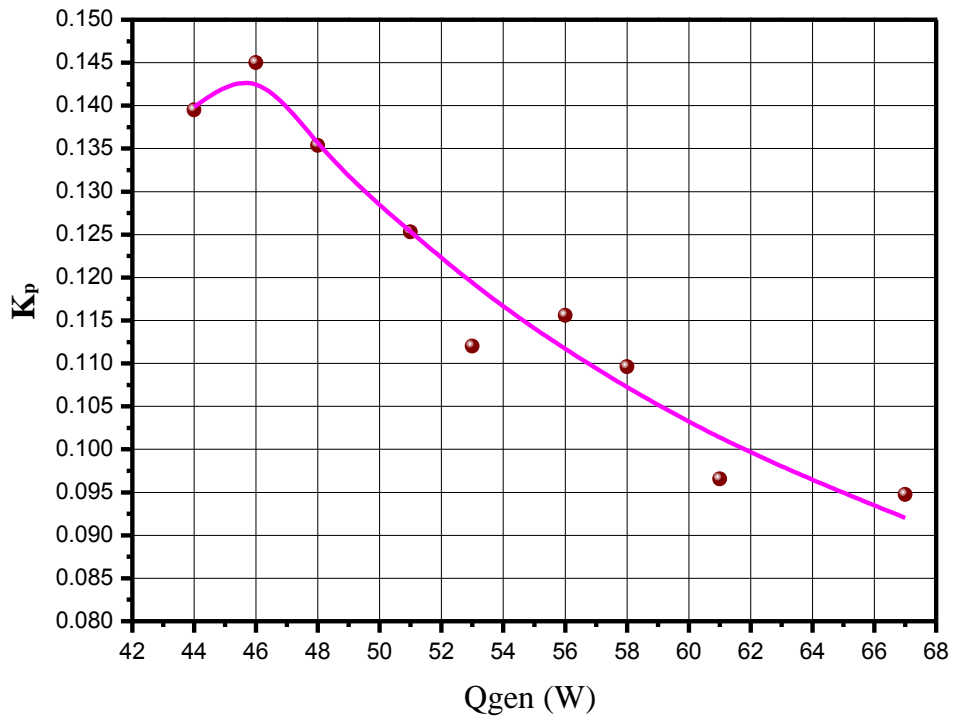
595

596

597

598

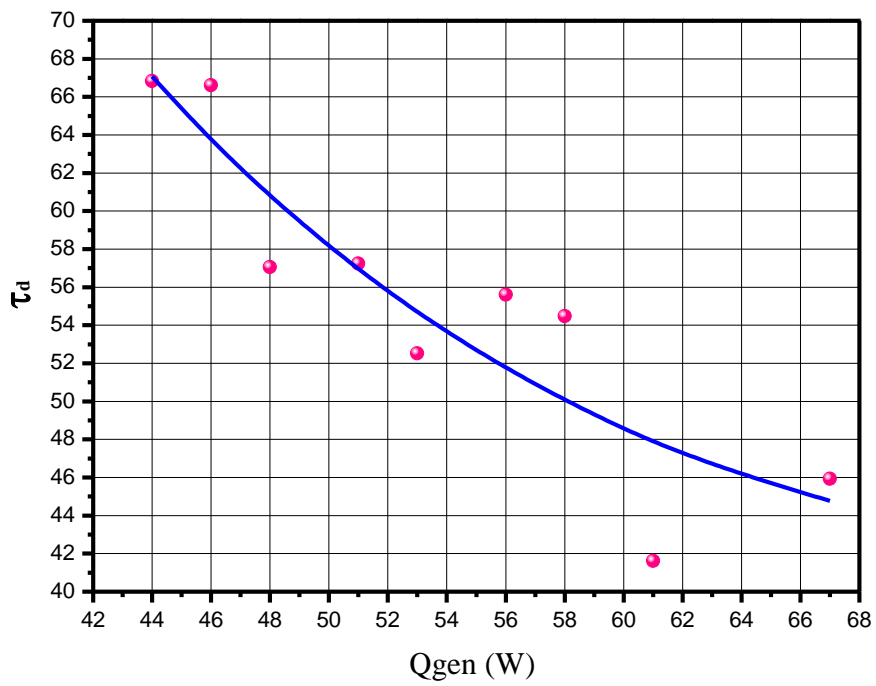
599



600

601

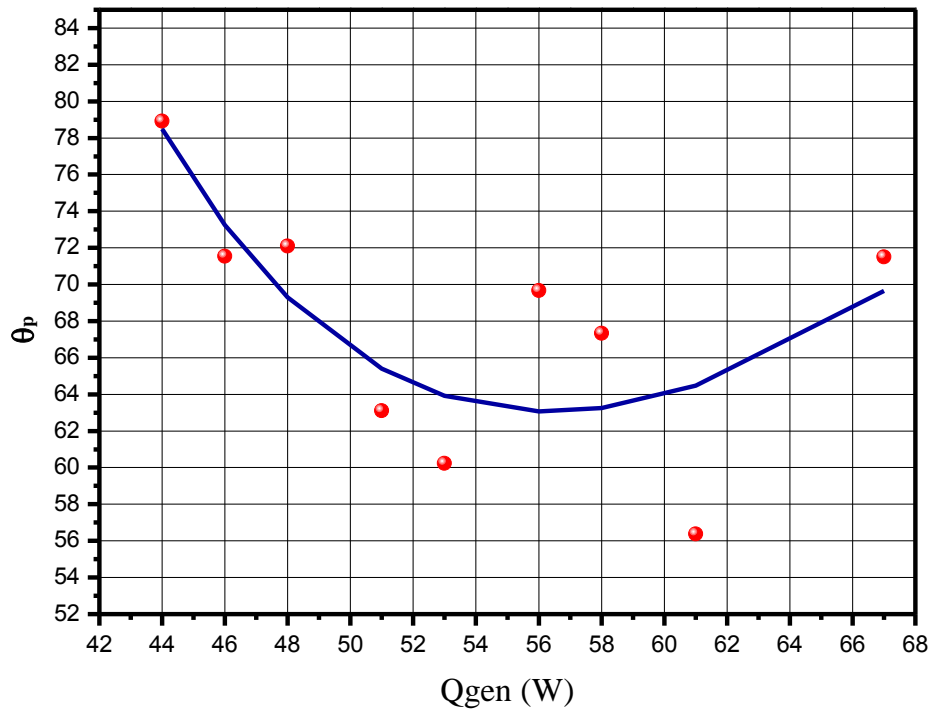
Fig. 8. K_p vs. \dot{Q}_{gen} .



602

603

Fig. 9. τ_d vs. \dot{Q}_{gen} .

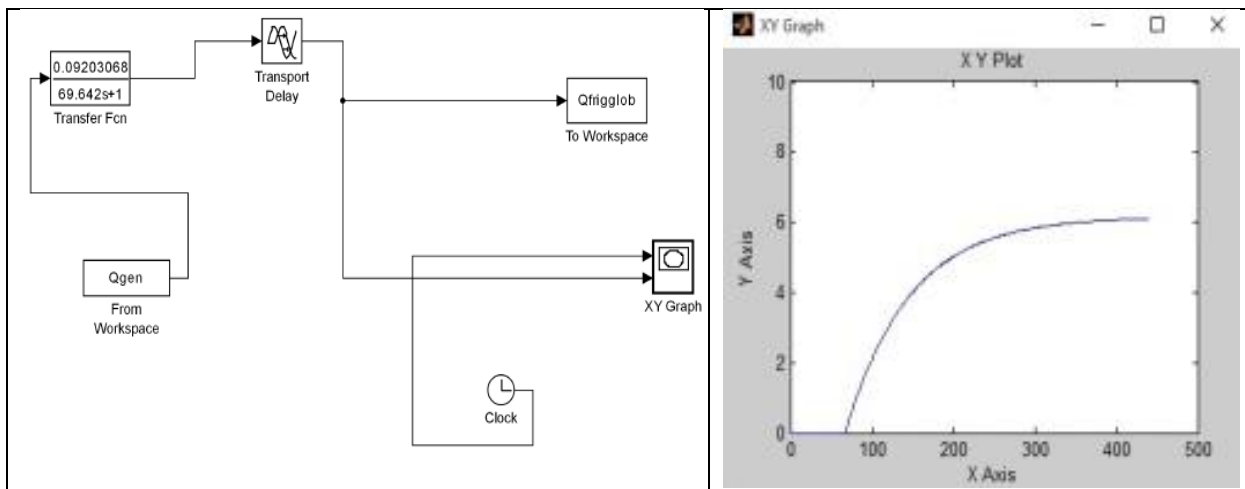


604

605

Fig. 10. θ_p vs. \dot{Q}_{gen} .

606



607

Fig. 11. Schematic diagram of the black-box dynamic model in the Matlab Simulink® environment.

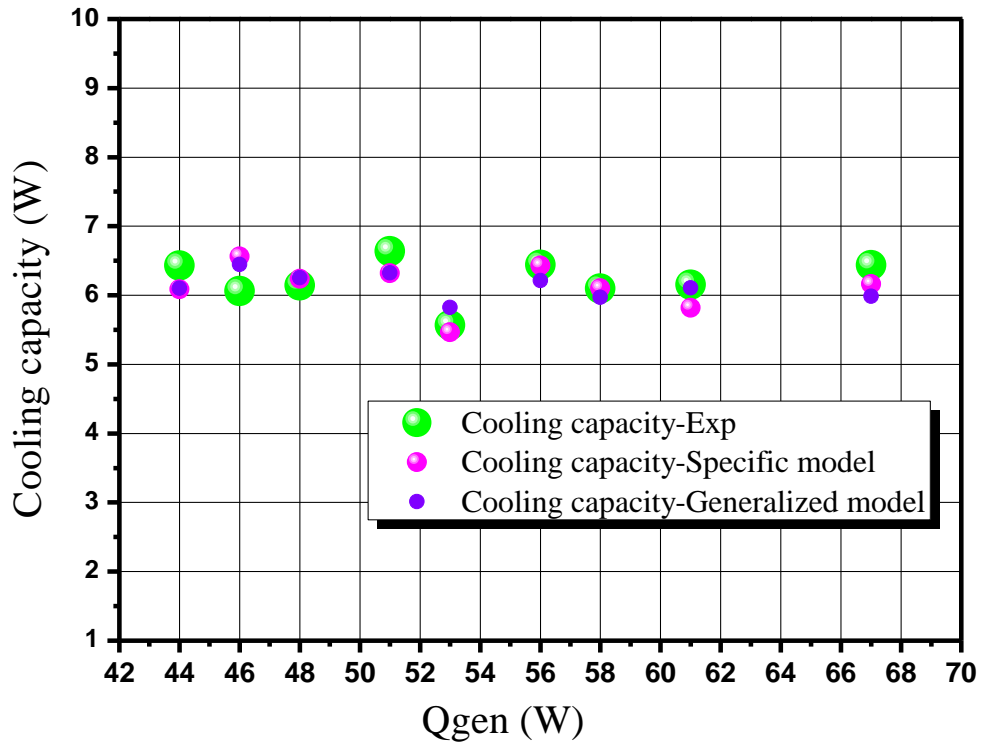
609

610

611

612

613



614

615 Fig. 12. Comparison of the experimental steady-state cooling capacity and that predicted by
 616 both the heat-rate-specific and generalized models as a function of the heat supply to the
 617 generator.